JOURNAL OF APPLIED ELECTROCHEMISTRY **29**: 209–219, 1999.

Quantitative phase analysis of galvannealed coatings by coulometric stripping

C. XHOFFER, H. DILLEN, B. C. DE COOMAN

OCAS N.V. (Research Centre of the Sidmar Group, Flat Products Sector of the Arbed Group), John Kennedylaan 3, B-9060 Zelzate, Belgium

A. HUBIN

Department of Metallurgy, Electrochemistry, Materials Science, V.U.B., Brussels, Belgium

Received 7 October 1997; revised 10 February 1998

The characterization of different Fe–Zn phases present in a galvannealed coating has been a challenging area of research in recent years. There have been doubts about the validity of the results obtained by electrochemical stripping because the data cannot be used for straightforward phase identification and because quantification needs to take into account the effect of various electrochemical side-reactions. The optimization of the electrochemical stripping method (also known as coulometric dissolution) and its use as a routine analysis method is reported. It is shown that the method allows the determination of the total Fe concentration, and the thickness and composition of the η, ζ, δ and Γ phases. Coulometric data obtained on a large number of TiNb interstitial free (IF) galvannealed samples were compared with the total iron and zinc concentrations determined by ICP-MS. Validation of the results was done by ICP–MS and EPMA. The coulometric method was verified on a large number of industrially produced galvannealed coatings and pilot line simulated galvannealed coatings.

Keywords: *coulometric stripping*, *Fe–Zn phases*, *galvannealed coatings*, *TiNb (IF) steels*

1. Introduction

Galvannealed coated steel sheet has found increased use in the automobile industry because of its superior resistance to corrosion, improved paintability and better weldability. The ductility of the coating depends strongly on the iron content and phase composition [1, 2].

Galvannealed coatings differ from pure Zn coatings in that they consist of a layered structure of different Fe–Zn intermetallic phases. Galvannealed coatings are produced by a continuous hot dipping process followed by an in-line annealing cycle, during which alloying takes place and the different Fe–Zn phases are formed. Industrial galvannealed coatings contain approximately 10% of iron by weight.

A galvannealed coating may consist of different intermetallic phases such as η, ζ, δ and Γ. There are still some uncertainties in the phase composition data, a general overview of which is given in Table 1. Often a further distinction is made for the δ phase into separate δ_{1k} and δ_{1p} phases, and for the Γ phase into separate Γ and Γ_1 phases [3, 4]. If the material is not fully alloyed, an η phase, consisting of Zn with a small amount of Fe in solid solution, is still present at the coating surface. The Γ phase is the most Fe-rich intermetallic phase in the coating. It is of special interest for coating adherence as it is the phase adjacent to the steel substrate. The higher the iron content in the coating, the poorer its formability. This embrittlement of the coating is mainly dependent on the iron content and the distribution of the different phases [1, 2].

Techniques such as EPMA [5, 6], XRD [7–10], TEM [11, 12], ICP-OES [13], SIMS [5], Mössbauer spectroscopy [7], light optical microscopy of colour etched cross sections [14–16] and electrochemical stripping [8, 10, 14, 15, 17] have been used to determine the Fe contents and thickness of the various phases in galvannealed coatings.

None of the above mentioned microanalytical techniques can easily determine the thickness or phase analysis of galvannealed materials because they are either limited in resolution, sample preparation and analysis time or because appropriate bulk galvannealed phase standards are missing.

Electrochemical stripping consists of the anodic dissolution of the coating at constant imposed current. The potential of the dissolving coating takes on a different value with respect to a reference electrode for each Fe–Zn intermetallic phase in the coating. Recording of the potential of the coating as a function of time makes it possible to determine the time, and thus the charge needed for a particular phase to dissolve anodically. This is why the technique is often referred to as coulometry.

Table 1. Fe (wt %) present in different galvannealed phases according to various literature sources

η (Zn)	ζ ($FeZn_{13}$)	δ ($FeZn_{10}$)	δ_1 ($FeZn_7$)	Γ_1 ($FeZn_4$)	Γ_1 (Fe_5Zn_{21})	Γ (Fe_3Zn_{10})	*Ref.*
			7.6–11.6				[3]
		8–13.5					[4]
<0.03	5–6	7–12		21–28			[18]
	5.2–6.1	7.0–11.5			16.6–21.2	15.8–27.7	[7]
	6.15	7.86	10.87				[19]
<0.1		6.3–11.5	6.3–11.5			20–27	[20]
<6	6.4		7–11.4			20–28	[20]
					16–21		[21]
	5.7–6.3						[22]
–	5.8–6.7		7.6–11.6		19.4–33.3		[23]
<0.03	5–6	7–12		16–21		21–28	[14]
	3		10		22		[15]
	6		9		17	21	[24]

According to several authors [8, 17, 25], the quantification of the different Fe–Zn phases present in galvannealed coatings is impossible because of the complex mechanisms and coupled electrochemical reactions taking place during stripping at constant current. It has been reported [17, 25] that a potential plateau observed during coulometric dissolution does not correspond uniquely to a particular Fe–Zn phase. Various phases will be attacked simultaneously during the anodic stripping. Zang and Bravo [25] reported that, at the start of coulometric dissolution, small crevices in the coating can be seen. These voids already exist in the coating as a result of thermal stresses during annealing and act as channels through which the electrolyte penetrates. The different phases are therefore exposed to the electrolyte from the start and can immediately be dissolved anodically. Different phases have different Fe-concentrations and different crystal structures. As a consequence, their dissolution rates at a certain potential are different.

There have also been contradictory reports on the effect of chloride ions in the electrolyte solution. According to Besseyrias *et al.* [8], chloride ions promote the corrosion by pitting and this results in the galvanic coupling between Fe-poor and Fe-rich zones. Zang and Bravo [25] have shown that chloride ions are necessary for promoting the resolution of the potential steps.

It is unclear whether the Fe present in the coating remains passive during electrolysis. It is possible that Fe dissolves partially and redeposits on the cathode. If Fe dissolves, corrections are used to compensate the charge consumed by the oxidation of iron.

A fundamental step in the phase recognition by means of a coulometric curve is that the final potential step corresponds to the iron dissolution of the substrate, whereas the penultimate plateau is a reorganisation plateau as a result from the Fe–Zn-coupling. Recently, some authors [5, 9, 15, 25] have reported that the penultimate plateau does not correspond to any Zn–Fe intermetallic phase and that it should be omitted in the phase calculations. Moens and Lamberigts [15] even proposed a way of calibrating coulometric stripping according to chemical analysis taking assumptions into account. The latter procedure and the assumptions were verified and further optimized resulting in the determination of the total Fe-concentration, the thickness and the phase composition of a galvannealed coating.

2. Instrumentation

Electrochemical measurements were performed with a potentiostat (model 273 EG&G) controlled by the EG&G corrosion measurement software M352. An electrochemical flat cell (EG&G model KO235) was used in combination with a Ag/AgCl reference and a Pt counter electrode.

All quantitative chemical analyses were performed on a VG Instruments high resolution ICP-MS. It is a double focusing mass analyser that ables high resolution mass separation whilst achieving high sensitivity.

X-ray microanalysis and morphology studies were done using a Jeol Superprobe 8800L equipped with a conventional EDX-detector and four wavelength dispersive detectors. EDX-analyses were performed using a 20 keV beam acceleration voltage and probe currents of about 1 nA.

3. Methodology

3.1. *Coulometric dissolution*

During a galvanostatic experiment, the sample is mounted in an electrochemical cell and a constant current is applied between the sample and the counter electrode. The metallic coating dissolves anodically. The potential of the working electrode changes to the potential that is necessary to maintain the specified current. Recording of the active potential with time results in a characteristic curve similar to that shown in Fig. 1. Each potential step corresponds to a different phase and the time required to dissolve a phase is determined using the second derivative of the coulometric curve. The relation between this time and the thickness of a particular Fe–Zn phase is determined by Faraday's law.

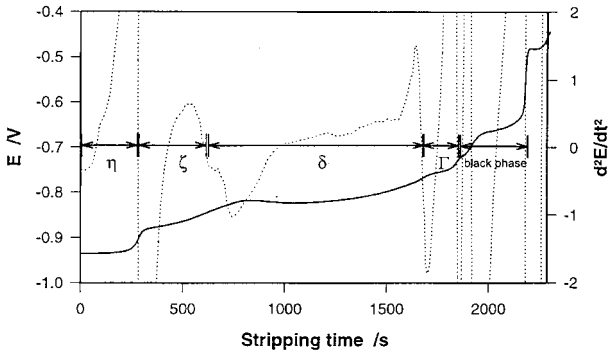

Fig. 1. Typical coulometric stripping curve of a nonfully alloyed galvannealed coating (—) and the second derivative of the curve for the determination of the time associated with the different phases (···). Key: (—) E; (·····) d^2E/dt^2.

Faraday's law can be applied to each intermetallic phase within the galvannealed coating:

$$d_i = \frac{M_i Q_i}{nFS\rho_i}\varepsilon_i \tag{1}$$

where:

d_i	coating thickness of phase i (cm)
M_i	molecular weight of phase i ($g\,mol^{-1}$)
Q_i	$i.t_i$, the number of coulombs required to strip phase i (C)
n	number of electrons exchanged
F	Faraday constant (96 485 $A\,s\,mol^{-1}$)
S	surface of the anode (cm^2)
ρ_i	density of phase i ($g\,cm^{-3}$)
ε_i	efficiency of the electrochemical stripping

Moens and Lamberigts [15] have proposed an original method for the analysis of coulometric data based on the following assumptions: (a) that the iron will not dissolve during the anodic dissolution; (b) that the total charge consumed by the electrochemical reaction is directly coupled to the Zn dissolution; and (c) that the H_2-evolution is a minor process and does not have to be taken into account.

As a consequence, the number of coulombs consumed during the stripping analysis is proportional to the Zn concentration in the specific phases. The Zn concentration (in $g\,m^{-2}$) in each phase i can then be calculated as

$$[\mathrm{Zn}]_i = \varepsilon_i \frac{Q_i}{AF}\frac{65.37}{2} = \alpha_i Q_i \tag{2}$$

and the total Zn concentration (in $g\,m^{-2}$) as

$$[\mathrm{Zn}]_{\mathrm{total}} = \sum_i \mathrm{Zn}_i = \sum_i \alpha_i Q_i \tag{3}$$

The coefficients α_i contain all the constants including the efficiency factor ε_i. For an efficiency of 100%, $\varepsilon_i = 1$, and $\alpha = 3.38$. The total Zn concentration can be determined by chemical analysis, making it possible to compute the regression coefficients, α_i, by least squares fitting.

The iron fraction can be calculated directly from the Zn concentration in each phase. If we assume that each intermetallic phase has a constant and known Fe composition, the Fe concentration (in $g\,m^{-2}$) for each phase is given by

$$[\mathrm{Fe}]_i = \%\mathrm{Fe}_i \alpha_i Q_i \tag{4}$$

Calibrating the α_i coefficients according to Equation 3, the wt % Fe as given in Equation 4 can be obtained by a least squares fitting to the total Fe values obtained by chemical analysis.

The total Fe weight can then be assessed by adding the Fe fractions of the different phases:

$$[\mathrm{Fe}]_{\mathrm{total}} = \sum_i [\mathrm{Fe}]_i = \sum_i \%\mathrm{Fe}_i \alpha_i Q_i \tag{5}$$

If the phase-specific Zn_i concentrations ($g\,m^{-2}$) and the corresponding wt % Fe_i are known, the thickness d_i of each intermetallic Fe–Zn phase can be calculated using the following expression:

$$d_i = \frac{\alpha_i Q_i}{10^6 \rho_{\mathrm{Zn}}} + \frac{\%\mathrm{Fe}_i \alpha_i Q_i}{10^6 \rho_{\mathrm{Fe}}} \tag{6}$$

where d_i is in μm.

3.2. *Gravimetry and ICP–MS analysis*

The total Fe and Zn content must be known for the determination of the α_i coefficients in Equation 3 and the Fe fractions in Equation 4. The total thickness allows for the verification of Equation 6. This information can be obtained combining gravimetric analysis with ICP-MS measurements.

The analysis is done using the following procedure: a 3 cm sized disc of the galvannealed material is cleaned with acetone and dried before weighing. The sample is then clamped into a holder of which the upper side (2.75 cm^2) is open. About 2 ml of acid solution (3.5 $g\,dm^{-3}$ hexamethylene tetramine in 6 M HCl) is brought in contact with the galvannealed material until the H_2-gas evolution stops. At that time, the galvannealed coating is dissolved and the solution can be transferred quantitatively into a 100 ml calibrated flask. The galvannealed material is dried and reweighed in order to obtain the dissolved weight fraction of the coating. The total coating thickness is given by the following expression:

$$d = \frac{10^4 W}{\rho S} \tag{7}$$

where d_i is the thickness of each intermetallic Fe–Zn phase (μm), W is the weight of the dissolved coating (g), ρ is the density of the galvannealed coating (7.25 $g\,cm^{-3}$) and S the dissolved area of the galvannealed coating (cm^2). The dissolved solution can be readily analysed for the elements Al, Fe and Zn by ICP-MS analysis using appropriate standard solutions.

4. Results and discussion

4.1. *Optimization of the coulometric conditions*

4.1.1. Electrolyte. Different electrolytes have been proposed for coulometric experiments for the deter-

mination of galvannealed phases. Zhang and Bravo [25] have used a 15–17.5% NaCl and 2.5–5% $ZnCl_2$ solution. The use of a 1 M Na_2SO_4 + 0.35 M $ZnSO_4.7H_2O$ solution [17] and a 200 g dm^{-3} NaCl + 100 g dm^{-3} $ZnSO_4.7H_2O$ solution [10, 14, 15] has also been reported.

Different electrolytes were evaluated by Hoet [26] and it was found that Cl-ions were necessary to obtain a better resolution of the potential jumps corresponding to the different phases. The Zn concentration must be high enough so that the Zn concentration in the solution remains constant according to the Nernst equation. Organic solutions must be avoided since the potentials measured are those of the organic components rather than those of the Fe–Zn phases. The best compromise was found for an electrolyte of composition 200 g l^{-1} NaCl + 100 g l^{-1} $ZnSO_4.7H_2O$. The same results can probably be obtained when the sulphate is replaced by $ZnCl_2$, but in this case, there is a risk of pitting by the Cl-ions.

To verify whether pitting is an important reaction during anodic dissolution of galvannealed coatings, coulometric stripping of various coatings as, for example hot dip galvanized, electrodeposited Zn and electrolytic Zn–Fe with different Fe wt % was performed. This was done using either a $ZnSO_4.7H_2O$ + NaCl electrolyte, a $(NH_4)_2SO_4$ solution or a buffer solution of citric acid. EPMA observations at different coulometric intervals show for all iron-rich coatings (galvannealed, electrodeposited Zn–Fe) the presence of cavities (crevices and channels). No differences in the galvannealing reaction and surface topography could be distinguished as a function of the electrolyte type. The cavities are not observed in pure Zn coatings (hot dip or electro deposited Zn).

4.1.2. Current density. The current density was optimized in the range 2–20 mA cm^{-2} to combine relatively short measurements and high stripping speed, while maintaining a good potential jump resolution. A current density of 7.5 mA cm^{-2} fulfilled both requirements [26].

4.1.3. Calculation of the potential steps times. For the identification of the different potential steps, the second derivative of the curve was calculated. The time between two successive changes of the second derivative from positive to negative values was taken as the phase specific dissolution time. This is illustrated in Fig. 1.

4.1.4. Intermetallic phase assignation in the electrochemical stripping curve. As stated earlier, there are still some contradictions in assigning the different potential steps for the various intermetallic Fe–Zn phases. One critical question is still unresolved. Should the last but one potential plateau be included [8, 10, 15, 17] or excluded [9, 14, 25] in the calculations? The coulometric dissolution curve of a galvannealed material was recorded using a NaCl electrolyte to answer this question (Zn was avoided since it would disturb the X-ray microanalysis). According to EPMA analysis [26, 27] and AES analysis [24], the η, ζ and δ phases are identified as indicated in Fig. 1.

During the coulometric dissolution of the different galvannealed phases, a black deposit is formed on the surface of the working electrode. This deposit becomes clearly visible during the dissolution of the δ phase. As long as the Γ layer is not dissolved, this black deposit cannot be removed from the surface. At the beginning of the second last potential plateau, the deposit can be removed by, for example, a soft water spray. At the end of the Γ dissolution plateau, the electrochemical stripping experiment was stopped and the black film was collected using a double sided conductive carbon tape. Quantitative EPMA analysis of the black deposit revealed a composition of approximately 59 wt % Zn (55 at %) and 41 wt % Fe (45 at %). A high oxygen signal was also observed in the deposit. The formation of the black layer could never be avoided by either heating of the electrolyte, rotation of the anode or by an electrolyte jet against the anode surface.

The penultimate potential plateau in the coulometric dissolution curve therefore results from complex electrolytic processes which lead to the black phase. Sometimes, these reactions result in very weak potential steps and associated second derivative changes, as seen in Fig. 1. During the black phase plateau, the Fe to Zn balance remains unchanged. From XRD and TEM studies, it is seen that the black phase is composed of a combination of different amorphous Fe and Zn rich oxides/hydroxides and possibly also metallic Fe. The deposit has an amorphous structure since no diffraction phenomena were observed with TEM and XRD.

Similar stripping experiments were done on electrolytically produced Zn–Fe coatings. The same phenomenon of the black deposit was observed giving the same Fe to Zn atomic ratios. No black deposit was observed on hot dipped galvanised or electrolytically produced Zn coatings. Only a grey colour at the surface was observed when the iron substrate was reached. The existence or growth of a black deposit during an electrochemical stripping process was dependent on the presence of Fe in the coating, and was therefore associated to crevices in the coating through which iron from the substrate can be dissolved. The number of coulombs corresponding with the black phase were not used in the calculations as they were not related to any Fe–Zn intermetallic phase.

4.2. *Determination of the α_i coefficients*

In these experiments, the phase-specific electrochemical parameters were determined by combining coulometry with chemical analysis. The Zn contributions deduced from the coulometric experiment were fitted to the Zn values obtained from ICP-MS measurements. The α_η or ε_η coefficient for the η phase can easily

be derived from hot dip galvanised material analysed under similar conditions as galvannealed material. The very low Fe concentrations present in the galvanised coatings ($< 0.25\,g\,m^{-2}$) can be neglected. Figure 2 shows a least square fitting of the Zn content determined by coulometry to the ICP-MS Zn content. For the η phase α_η was calculated to be 3.52.

For the determination of α_η, α_ζ, α_δ and α_Γ, coulometric analysis and ICP-MS determinations for Zn and Fe were carried out on a large number of galvannealed coatings. The least square fit for surface specific Zn weight according to the linear model introduced earlier in Equation 3 is presented in Fig. 3. The calculated α_i values are given in Table 2. These coefficients were then used for the calculation of the corresponding wt % iron in the different phases by applying Equation 5. The result of the least square fit for iron is given in Fig. 4. A linear correlation coefficient of almost 95% was obtained. The iron weight percentages for the different phases are also listed in Table 2.

The total thickness of a galvannealed layer can be derived from the stripping experiments using Equation 6 and the α_i coefficients. The plot of the total thickness estimated by coulometry against the thicknesses determined by gravimetry is shown in Fig. 5. A very good correlation coefficient of more than 95% is obtained suggesting that the obtained electrochemical coefficients (α_i) as determined by ICP-MS calibration can be used to characterize galvannealed coatings.

Values of $\varepsilon > 1$ mean that more Zn is measured than calculated according to Faraday's law. This means that besides anodic reactions, cathodic reactions also take place at the anode. The most probable cathodic side-reaction is hydrogen evolution, which is visible during the dissolution and galvanic corrosion.

Values of $\varepsilon > 1$ indicate that less Zn is oxidized than according to Faraday's law. This is an indication that other anodic reactions such as iron dissolution, are taking place simultaneously.

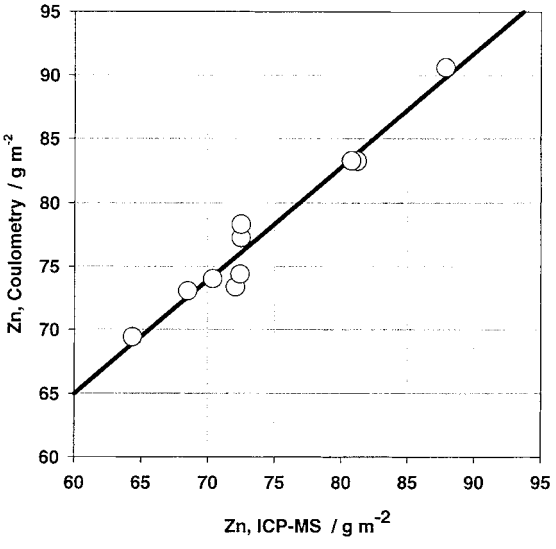

Fig. 2. Least squares fitting of the coulometric surface specific Zn weight ($g\,m^{-2}$) to the surface specific Zn weight determined by ICP-MS for hot dip galvanized coatings.

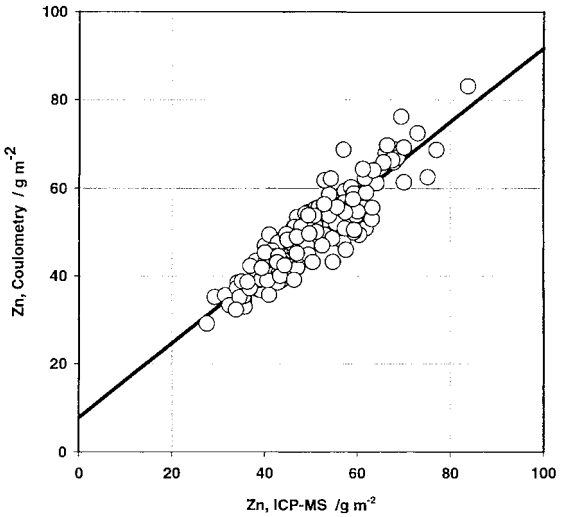

Fig. 3. Least squares fitting of the coulometric surface specific Zn weight ($g\,m^{-2}$) to the surface specific Zn weight determined by ICP-MS for galvannealed coatings.

Finally, it is the balance between all possible reactions (Zn dissolution, Fe dissolution and cathodic reactions) that determine the final value of ε. From the ε coefficients of the δ and Γ phases, cathodic side reactions can be very large resulting in overall side-reactions of more than 20% of the total dissolution reactions.

The results obtained for the phase compositions (Table 2) are in very good agreement with the EPMA results obtained from standards [24]. The results also correspond very well to the expected values of a galvannealed coating. For example, in a fully alloyed coating, no η phase is present and beside the small ζ contributions, the δ phase represents the major iron constituent. As the total iron content should be around 10% by weight, the total iron content will be balanced by the presence of the iron richer Γ fraction.

In general, for electrochemical stripping experiments performed on galvannealed coatings, the Fe and Zn concentrations as well as the thickness of each phase can be calculated according to Table 3.

4.3. *Mechanism of anodic dissolution during coulometric experiments*

The precise mechanism of anodic dissolution during the coulometric experiments is still unclear. Lamb-

Table 2. Electrochemical dissolution coefficients (α_i), efficiency factors (ε_i) and iron weight fractions (wt % Fe) for the different specific galvannealed phases

Phase	ε	α_i	*wt % Fe*	*EPMA (wt % Fe)**
η	1.04	3.519	0.0	
ζ*	0.90	3.057	4.1	6
δ	1.21	4.100	9.2	9
Γ	1.17	3.942	18.2	17

* In a recent dissertation manuscript [24], EPMA and Auger microanalysis were done on standard galvannealed powder materials that were prepared by controlled thermal analysis.

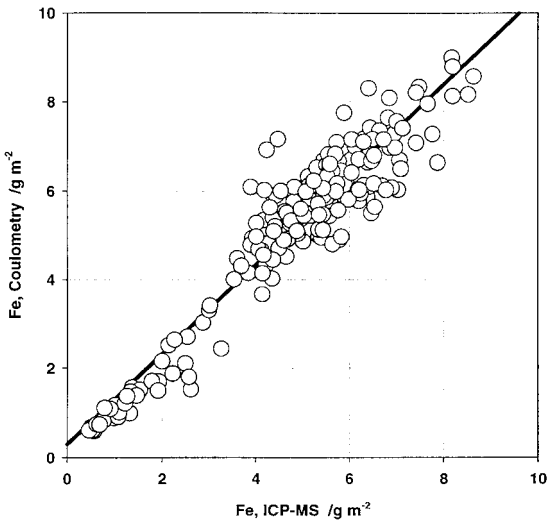

Fig. 4. Least squares fitting of the coulometric surface specific Fe weight ($g\,m^{-2}$) to the surface specific Fe weight determined by ICP-MS for galvannealed coatings.

erigts *et al.* [14] suggest that the coating is dissolved layer by layer and that only Zn and no Fe is oxidized. Moreover, they propose that no hydrogen evolution occurs. Van Heusden [27] has shown that small cracks, extending towards the steel substrate, are present at the surface of the coating. Such crevices exist due to thermal stresses which occur in the coating as a result of the annealing. The layer by layer dissolution theory is questioned by others [8, 17, 25] on the basis that Zn is preferentially dissolved. The electrolyte penetrates deep into the coating, and all layers are simultaneously in contact with the electrolyte and oxidized. The layers have different Fe concentrations and consequently different dissolution rates, making the coulometric response complex.

Essential in the comparison of the two opinions was the characterization of the surface modification which takes place during anodic dissolution. The coulometric experiment was therefore interrupted at

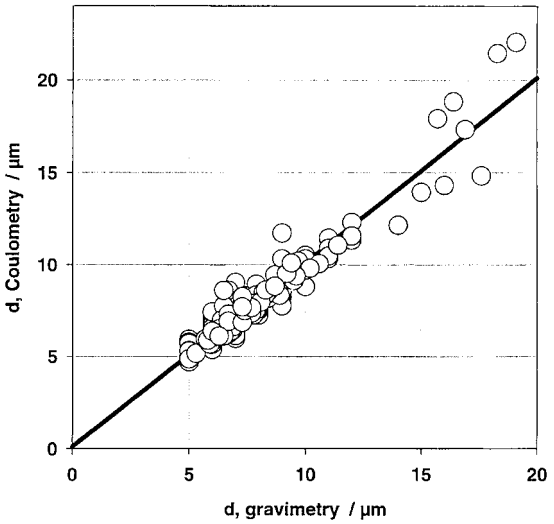

Fig. 5. Total thickness of galvannealed coatings as determined by electrochemical stripping and gravimetry.

Table 3. Formulae for direct calculation of the weight specific Zn and Fe concentrations, as well as the thickness of each intermetallic Fe–Zn phase

i is the applied current density ($A\,cm^{-2}$) and t_i is the phase specific dissolution time (s)

Phase	*Thickness*/µm	*Zn conc.*/$g\,m^{-2}$	*Fe conc.*/$g\,m^{-2}$
η	$0.493\,it_\eta$	$3.519\,it_\eta$	0
ζ^*	$0.429\,it_\zeta$	$3.057\,it_\zeta$	$0.0126\,it_\zeta$
δ	$0.621\,it_\delta$	$4.100\,it_\delta$	$0.3776\,it_\delta$
Γ	$0.638\,it_\Gamma$	$3.942\,it_\Gamma$	$0.7163\,it_\Gamma$

different representative points and a combined surface analytical (with SEM and EDX) and chemical (with ICP-MS and gravimetry) study was carried out.

For each stripping time, a SEM picture of the surface was taken. An EDX analysis on different spots distributed over the surface and an EDX mapping of Fe and Zn was done. By doing so, information on the homogeneity of the dissolution process was obtained. Moreover, for each stripping time the electrolyte, the deposit on the counter electrode and the black deposit were also analysed by ICP-MS. This gave information on the composition and thickness of the different layers of the coating. Finally, with a combined gravimetric/ICP-MS analysis of the global coating, the total amounts of Zn and Fe and the thickness of the coating were determined.

4.3.1. Surface analytical characterization of the coating structure. On each sample, a SEM image was taken and EDX analyses were obtained on 10 different areas. The SEM images are shown in Fig. 6. The mean values and standard deviations of the Zn and Fe concentrations on the different samples are listed in Table 4. In Table 4, measurement 1 was made on the as-produced surface which consisted mainly of ζ phase crystals. Points 2 and 3 are located within the δ layer and points 4 and 5 correspond to the beginning and end of the Γ layer, respectively. Points 6 and 7 are representative for the surface and middle of the black layer. The reason for the somewhat higher Fe concentrations (and consequently lower Zn concentrations) in the δ and Γ phases can be due to the accumulation of the black deposit at the surface of the working electrode. Characteristic X-ray contributions of the underlying substrate is also a factor which will enhance the Fe X-ray intensity.

The SEM images show that the cracks, initially present, expand continuously during the coulometric experiment. They gradually form deeper and broader channels.

The SEM pictures clearly show a growing porosity of the dissolving coating. It is conceivable that small parts of the coating might fall off and end up in the electrolyte. A full electrolysis was therefore carried out. The electrolyte was filtered over a 0.05 μm filter and rinsed with hot water. The filter was then inspected by EPMA and the absence of any type of metallic parts confirmed. Hence, the growing porosity

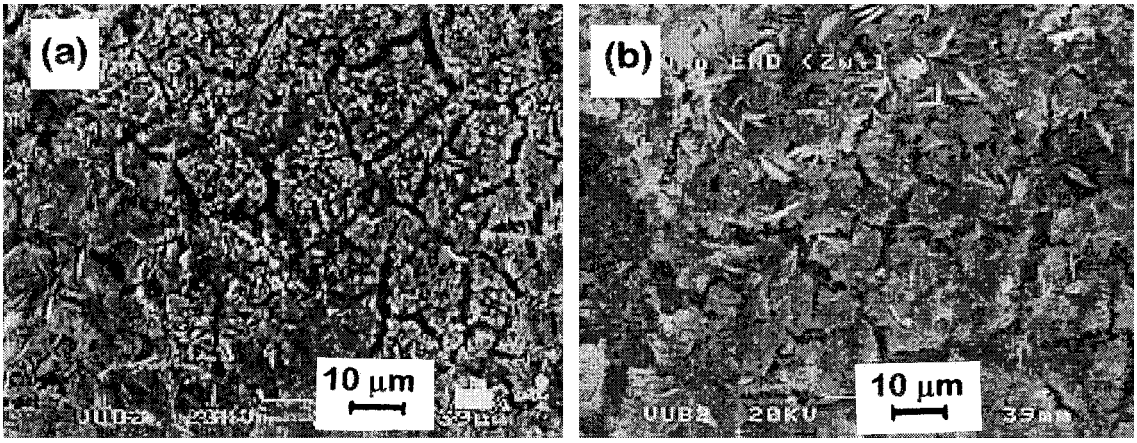

Fig. 6. Secondary electron images recorded from partially stripped intermetallic Fe–Zn layers of a galvannealed coating taken at the start of the Γ-potential plateau (a) and at the start of the black layer potential plateau (b).

does not result in Fe rich particles falling in the electrolyte.

At the start of the coulometric experiment, an Fe content of 9% by weight was found. This was somewhat higher than the Fe concentration of the ζ phase. While progressing in the dissolution of the δ layer, the Fe amount increased to a value of about 20% towards the end of the δ plateau. The enrichment in Fe continued in the Γ layer, where the amount increased to approximately 35%. In the black layer, the Fe content reached a constant value of approximately 52%. The amount of Fe and the standard deviation on the measurements increased, indicating that Fe is not homogeneously distributed over the surface.

4.3.2. Chemical analysis of the coating by electrolyte compositional changes. A chemical analysis of the electrolyte was carried out for both the layer by layer and the global stripping to find out which components were dissolved during the coulometric experiment. After each interruption, the electrolyte and the deposit on the counter electrode and the black deposit were collected and analysed with ICP-MS.

For this experiment, a 0.05 M NaCl electrolyte was used instead of the conventional solution for two reasons. First, the conventional electrolyte contained a Zn concentration which is too high. The very small Zn dissolution contribution from the electrochemical stripping could not be determined accurately. Secondly, the high NaCl concentration in the conventional electrolyte caused problems during the introduction of the solute in the nebulization and atomization chambers of the ICP-MS.

The counter electrode deposit was dissolved in a small volume of 0.01 M HCl and analysed. At the end point, the black deposit on the working electrode was dissolved in a solution of $3.5\,g\,dm^{-3}$ hexamethylene tetramine in 6 M HCl and analysed.

The ICP-MS results of this differential stripping are given in Tables 5 and 6. Table 5 gives estimates of the fractions of the stripped material as determined by the analysis of the electrolyte and the counter electrode. In Table 6, the total of all fractions of the electrochemically stripped material are compared with the gravimetrically obtained results.

4.3.3. Chemical analysis related to the global coating. The procedure was as described earlier. The electrolyte was analysed by ICP-MS after dissolution of the coating, and the analysis was combined with gravimetry to obtain the Zn and Fe concentrations and the thickness of the coating.

The results are also given in Table 6, together with the total thickness and the total amounts of Zn and Fe obtained by summation of the data of the sublayers of Table 5.

4.3.4. Discussion. The SEM-EDX data in Table 4 show that, compared to the literature data listed in

Table 4. X-ray microanalysis results of a differential stripping experiment

Position on the i/t curve	*Phase*	*Fe*		*Zn*	
		/wt %	std dev.	/wt %	std dev.
1	ζ	9.0	0.3	90.1	0.4
2	δ	12	1	87	1
3	δ	22	5	77	4
4	Γ	34	8	65	7
5	Γ	37	5	61	5
6	black layer	52	3	46	3
7	black layer	53	3	44	3

Table 5. ICP-MS results of the differential coulometric stripping of a galvannealed coating

Electrolyte and counter electrode concentrations are recalculated to the coating specific fractions

Stripping time /s	*Thickness* /μm	*Electrolyte concentrations*			Counter electrode	
		/g m^{-2} (Fe)	/g m^{-2} (Zn)	/wt % (Fe)	/g m^{-2} (Fe)	/g m^{-2} (Zn)
342	1.9	1.5	12.5	10.7	0.017	0.707
684	1.5	1.3	9.8	11.7	0.001	0.468
1026	1.2	1.4	7.2	16.2	0.001	0.463
1240	0.8	1.2	4.6	20.2	0.001	0.481
1560	0.8	1.5	4.4	25.5	0.001	0.469
1860	0.7	1.6	3.3	32.3	0.001	0.425
2083	0.6	2.6	1.6	62.1	0.001	0.123

Table 1, higher Fe concentrations are found for the expected Fe–Zn intermetallic compounds. The enhanced Fe concentration may be due to three phenomena:

(a) Only Zn is oxidized during coulometry, and Fe remains strongly enriched at the surface.
(b) Element specific X-ray intensities arise also from the underlaying layers because of the escape depth of X-rays.
(c) Side reactions take place. This is also suggested by the values of ε listed in Table 2.

A very good balance for the total Zn content can be observed when comparing the results of the layer by layer stripping and the global stripping in Table 6. For Fe, however, the content recovered in the different steps is twice as high as the one found in the coating only. Moreover, the thickness of the stripped material is 0.7 μm higher than the one calculated from the gravimetric experiment. The reason for the discrepancies between the total Fe content in the coating and the total coating thickness can only be due to the partial dissolution of the steel substrate during the anodic stripping process. This process can take place at the crevices that are inherently present in an alloyed Fe–Zn layer. Due to this phenomenon, the Fe content of the layers cannot be measured directly from the coulometric experiment. It can indirectly be derived from the coulometric data, since the correction coefficients take the side reaction of the substrate dissolution into account. From this experiment it is clear that the hypothesis that only Zn is oxidized is not valid.

The ICP-MS results of the differential coulometric stripping experiment given in Table 6, are presented in Fig. 7 together with the predicted values calculated by the proposed coulometric method and the theoretical values based on Faraday's law. The curves presented in Fig. 7(a) are accumulated values for the surface-specific Zn concentrations (g m^{-2}). The line indicated by fractionated ICP-MS are the measured Zn concentrations in the electrolyte added to the fraction deposited onto the counter electrode. The concentrations (expressed in g m^{-2}) are recalculated from the specific dissolved area of 1 cm^2.

At the beginning of the experiment, the slope of the ICP-MS curve is the same as the coulometric curve. As the dissolution process evolves, the ICP-MS slope decreases as the black phase grows in thickness. Calculations based on Faraday's law underestimate the Zn concentrations, indicating that additional currents must be taken into account. The difference between the coulometric curve and the ICP-MS measurement is exactly balanced by the fraction of Zn measured in the black phase.

From the curves, it can be seen that the rate of Zn dissolution diminishes slightly as a function of time corresponding to the stripping of the successive phases which are poorer in Zn. The last point in the ICP-MS curve corresponds to the penultimate plateau in the coulometric curve and has therefore no analogue in the other curves.

During the stripping experiment, much higher Fe values were measured in the electrolyte and counter electrode than theoretically possible if only coating dissolution occurs. The actual Fe concentration measured in the electrolyte is an accumulation of the Fe from the coating added to the Fe dissolved from the substrate.

During the coulometric experiment, various electrochemical and chemical processes are taking place simultaneously. The mechanism of Zn and Fe dissolution by electrochemical stripping can be visualized by the schematic shown in Fig. 8. Suppose the galv-

Table 6. Estimated thickness and specific coating weights of the collected fractions during coulometric stripping of a galvannealed coating

	Thickness /μm	/g m^{-2} (Fe)	/g m^{-2} (Zn)	/wt % (Fe)
Total electrolyte	7.5	11.1	43.4	20.4
Total counter electrode	0.5	0.02	3.2	0.7
Black deposit	1.2	3.04	5.5	35.7
Total all fractions	9.2	14.2	52.1	21.5
Gravimetry + ICP-MS	8.5	7.1	54.0	11.6

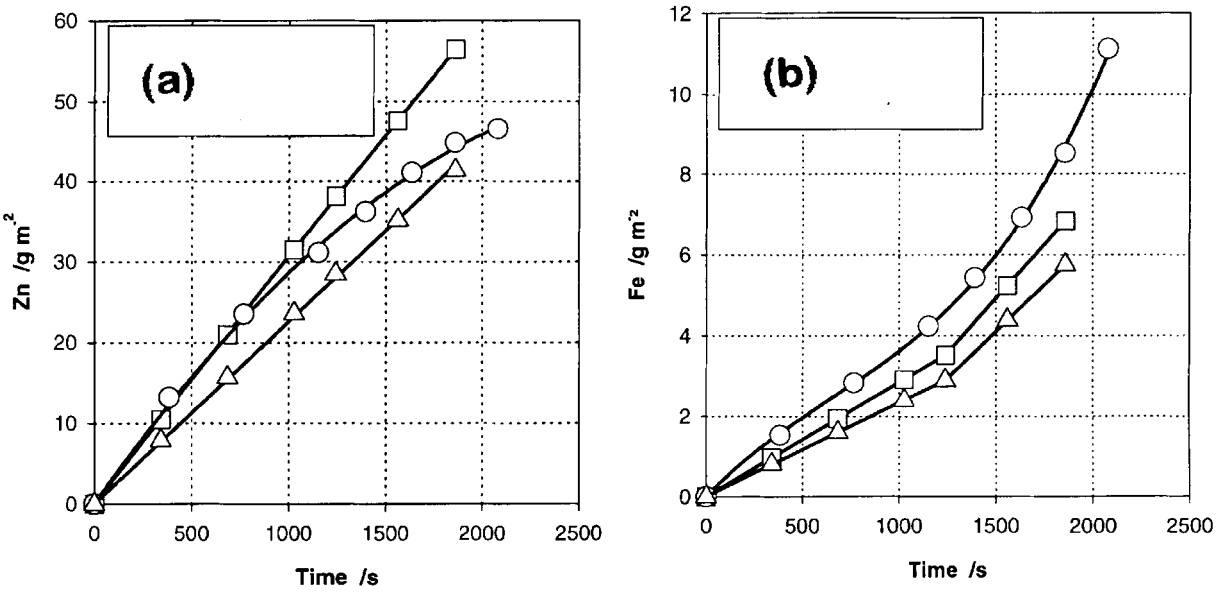

Fig. 7. Results of Zn (a) and Fe (b) in the electrolyte as determined by the combination of differential coulometry with ICP-MS. Key: (□) coulometry, (○) fractionated ICP-MS and (△) Faraday's law.

annealed coating is composed of a δ and Γ layer in which crevices are present. At the beginning of the electrolysis, Zn oxidation occurs (Fig. 8(a)). As the electrolysis proceeds, the surface becomes poorer in Zn. Fe accumulates at the surface (indicated by the dashed areas), partially inhibiting further Zn dissolution. Fe dissolution becomes a competitive side reaction. Because the oxidation of Fe consumes a part of the opposed current, the dissolution rate for Zn is smaller than given by Faraday's law. This results in α_i factors that are smaller than the theoretical value of 3.38 according to Faraday's law, and the efficiency of the electrochemical stripping (ε) will be smaller than one. Since the experimentally derived ε values for both the δ and Γ phases are much larger than one, other, more important side reactions are active.

Because of galvanic coupling, Zn will be oxidized by the reduction of Fe. Metallic Fe fractions will be redeposited onto the surface. This indirect reaction by galvanic coupling does not disturb the applied current and therefore does not interfere with the electrochemically derived calculations.

Within the crevices of the coating there is almost no turbulence of the penetrating electrolyte. Under such static conditions, natural galvanic corrosion can occur. Corrosion is assumed to be controlled by the combined reduction of water and oxygen [28]. The reduction of dissolved oxygen is diffusion controlled because of the limited solubility at room temperature. The reduction of water to H_2 is activation controlled because of the unlimited supply of water molecules. Both competitive reactions are suppliers for hydroxide ions (Fig. 8(b)). The deposition of Fe and Zn hydroxides at the surface of the coating is very likely.

Hydrogen evolution occurs as the result of the galvanic coupling between Zn rich and Fe rich phases. On the microlevel, during anodic dissolution, cathodic reaction zones at the coating surface and in the voids are formed where hydrogen reduction takes place. This leads to an induced current as the result of galvanic corrosion that needs to be taken into account with the electrochemical imposed current. Hydrogen evolution results in efficiency factors larger than one.

In the presence of chloride ions, even at pH 6.5, other side reactions of Zn^{2+} and Fe^{2+} are possible (Fig. 8(c)) [29, 30]. Such side reactions can take place at very localised areas at the coating surface. In these side reactions, the protons formed can either recombine with the hydroxide ions, or promote further dissolution of the Zn and Fe fractions, thus giving ε values larger than one.

The experimentally derived efficiency factors (ε_i) as given in Table 2, are the result of all these side reactions, indicating that the overall effect contributes more than 20% to the opposed current. According to this model, simultaneous dissolution of the intermetallic sublayers can only take place through the crevices. Since the surface active area within these crevices is small, compared to the total dissolution area, the δ and Γ phases will dissolve separately. This is also indicated by the potential step observable between the δ and Γ phases.

4.4. *Industrially processed and pilot line simulated Ti and Nb alloyed interstitial free (IF) substrates*

Based on the coulometric parameters determined by calibration with respect to ICP-MS results, more than 180 industrially processed galvannealed coatings on Ti–Nb IF materials were characterised by coulometric stripping analysis. The phase specific characteristics of the galvannealed coatings such as thickness, iron and zinc weights, were determined using the electrochemical parameters listed in Table 2. The results of the industrially galvannealed coatings on Ti–

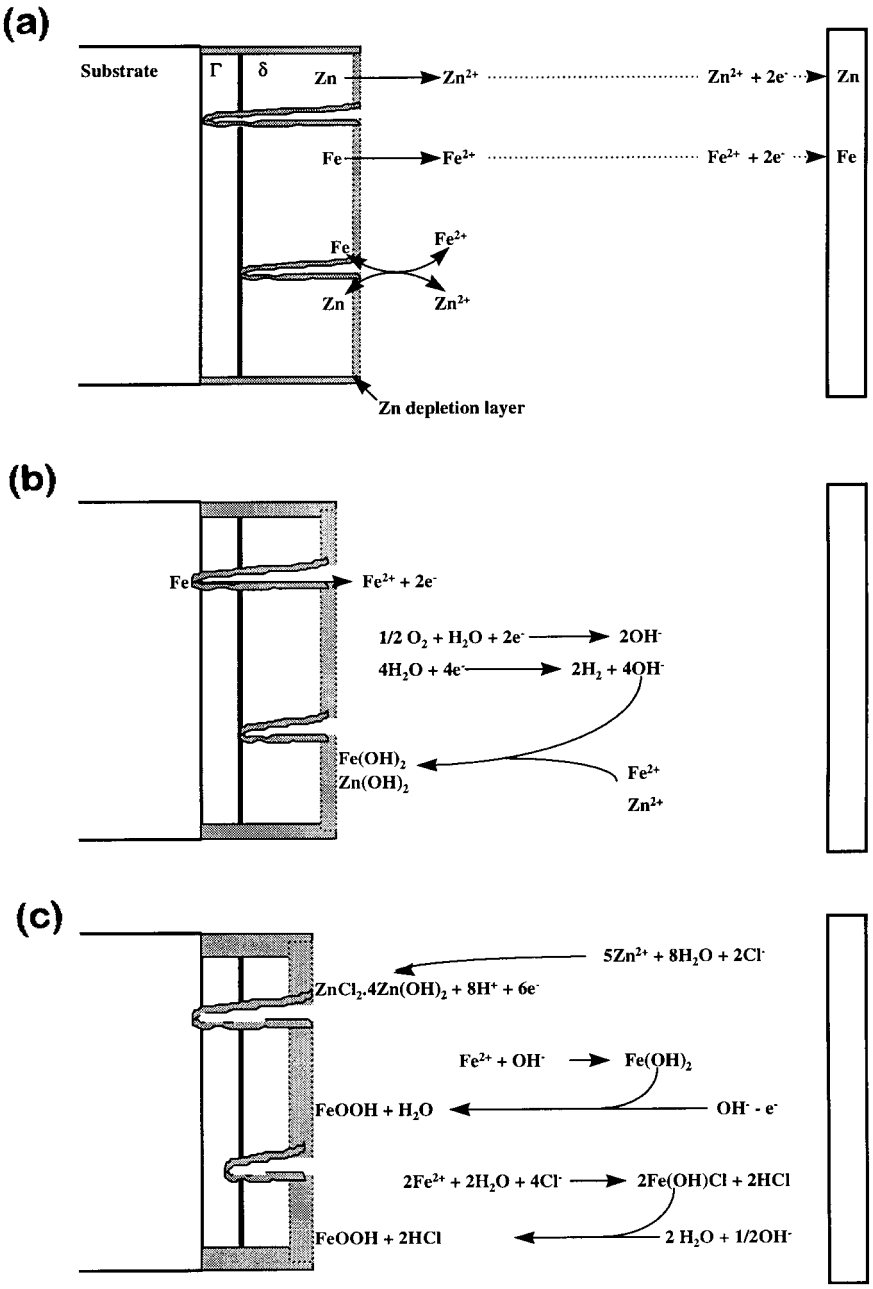

Fig. 8. Schematic showing the different reactions taking place during the coulometric stripping of a galvannealed coating. The dashed area is enriched in Fe.

Nb IF substrates are shown in Fig. 9(a). The data illustrate that for increasing iron contents (up to 8%), both the η and ζ phases rapidly decrease, favouring the growth of the δ phase. With further increase in iron concentration above 9%, the Γ phase grows at the expense of the δ phase. Only a few of the industrially processed materials, show the presence of an η phase.

Together with the industrially processed substrates, about 56 pilot line simulated galvannealed coatings on TiNb IF substrates were analysed. The large variations in processing conditions made it possible to observe the phase transformations as a function of iron content in the coating. The results of the coulometric analysis are shown in Fig. 9(b).

It is surprising to see that the gamma layer thickness remains constant in the range 5% to 8% Fe. For iron concentrations between 9 and 10% by weight, an increase in gamma thickness is observed. The curves 9 (left and right) match perfectly in overlay, showing that the phase characterization is consistent within the full range of alloying grades.

In the case of Ti–Nb IF coated substrates that have been deformed, more and/or larger crevices can occur and this may influence the rate of the various side reactions thus leading to different results.

5. Conclusions

The applicability of coulometric stripping for the phase analysis of galvannealed coatings was tested and optimized. The coulometric results were fitted to the total Zn and Fe concentrations as determined by ICP-MS using regression analysis. The combination

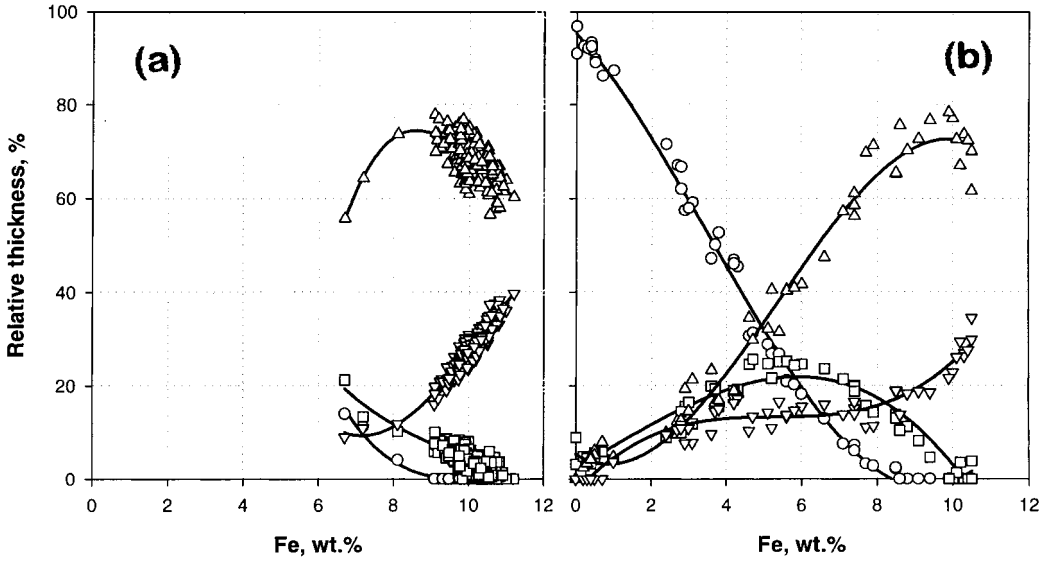

Fig. 9. Coulometric analysis performed on industrially processed galvannealed Ti–Nb substrates (a) and pilot line simulated galvannealed Ti–Nb substrates (b). Key: (○) η, (□) ζ, (△) δ and (▽) Γ.

of coulometry with EPMA was used for the phase recognition of the coulometric curves. Different microanalytical techniques were used to gain insight into the electrochemical reactions, as well as the major side-reactions. The overall effect of the various side reactions contribute to more than 20% of the total electrochemical reactions. They are particularly important during the dissolution of the δ and Γ phases.

The coulometric curve gives reliable data on the thickness and composition of the different layers, on the condition that (a) the part of the curve representative of the black layer is discounted and (b) a correction, taking into account the various side reactions, is made. Coulometry was used successfully for the characterization of galvannealed coatings on Ti–Nb IF substrates produced either industrially and on a pilot line.

The coulometric dissolution method and the proposed data analysis method can be used for the characterization of both the thickness and the intermetallic phase content of galvannealed coatings.

References

[1] G. Claus, J. Dillewijns, B. C. De Cooman, and U. Meers, Galvatech '95 Conference Proceedings, 17–21 Sept., Chicago, IL, (1995), p. 107.

[2] G. Claus, J. Dillewijns, H. Storms, J. Scheers and B. C. De Cooman, *La Revue de Metallurgie-CIT*, June (1995) 805.

[3] M. A. Ghoniem and K. Lohberg, *Metall* **26** (1972) 1026.

[4] H. Ohtsubo, T. Yagi, K. Nakai and Y. Ohmori, *ISIJ International* **36** (1996) 317.

[5] W. van Koesveld, M. Lamberigts, A. van der Heiden and L. Bordignon, Galvatech '95, *op. cit*. [i], (1995), p. 343.

[6] C. S. Lin and M. Meshii, *Metall. Materi. Trans B* **25** (1994) 721.

[7] D. C. Cook and R. G. Grant, Galvatech '95, *op. cit*. [i], (1995), p. 497.

[8] A. Besseyrias, F. Dalard, J. J. Rameau and H. Baudin, *Corrosi. Sci.* **37** (1995) 587.

[9] P. Angermayer, M. Mayr, J. Angeli and J. Faderl, *Z. Metallkd.* **84** (1993) 716.

[10] S. Mathieu, 'Colloque: Methodes d'Investigation des Métaux', St-Etienne, 3 Déc. (1980).

[11] Y. Lin, W. Chiou and M. Meshii, Atomic Structures of Interfaces in Annealed Electrogalvanized Steel Sheets, Galvatech '92; Second International Conference on Zinc and Zinc Alloy Coated Steel Sheet, Amsterdam, The Netherlands, 8–10 Sept. (1992), p. 429.

[12] L. A. Giannuzzi, P. R. Howell, H. W. Pickering and W.R. Bitler, Interfacial characterization of Zinc-coated Steels by TEM: A Preliminary Study, Zinc-Based Steel Coating Systems: Metallurgy and Performance, edited by G. Krauss and D. Matlock (The Minerals, Metals & Materials Society, 1990), p. 121.

[13] J. Symonds, 45th Chemists' Conference, Research and Developmemt Department Britisch Steel, Royal Hotel Scarborough, 15–17 June (1993).

[14] M. Lamberigts, J. P. Servais and E. Moens, CRM Metal Science Report, SM 190, S 6/93 Liège (1993).

[15] E. Moens, M. Lamberigts, CRM Metal Science Report, SM 210, S 5/94 Liège (1994).

[16] J. R. Kilpatrick, *Pract. Met.* **28** (1991) 649.

[17] H. Baudin, A. Besseyrias, F. Dalard and J. J. Rameau, Galvatech '92; *op. cit*. [ii], (1992), p. 455.

[18] A. Stadlbauer, F. Rubenzucker, K. Zeman, E. Fuhrmann, J. Faderl and L. Schonberger, Galvatech '95, *op. cit*. [i], (1995), p. 81.

[19] M. Hansen and K. Anderko, 'Constitution of Binary Alloys' (McGraw-Hill, New York, 1958), p. 737.

[20] J. Schramm, *Z. Metallkunde* **7** (1936) 203.

[21] G. F. Bastin, F. J. J. van Loo and G.D. Rieck, *ibid.* **10** (1974) 656.

[22] P. J. Gellings, E. W. de Bree and G. Gierman, *ibid.* **5** (1979) 315.

[23] L. Meyer *et al*., 'Metallk. Analyse', Wien (1969).

[24] B. Charot, Dissertation (Vrije Universiteit Brussel, Brussels, 1995).

[25] X. G. Zhang and I.C. Bravo, *Corrosion* **50** (1994) 308.

[26] G. Hoet, Dissertation (KHIH West-Vlaanderen, Oostende, 1995).

[27] W. Van Heusden, Dissertation (Vrije Universiteit Brussel, Brussels, 1996).

[28] D. A. Jones and N. R. Nair, *Corrosion Nate* **41** (1985) 357.

[29] D. Massion and D. Thierry, *in* 'Automotive Corrosion and Protection', edited by R. Baboian, Proceedings of the Corrosion' 91 Symposium (1992), pp. 10–11.

[30] W. Schwenk, *in* 'Korrosionsschutz durch Information und Normung Verlag I. Kuron', Scftenreihe der Arbeitsgemeinschaft Korrosion e.V. (W. Fischer (Hrzg.), 1988), p. 147.